

# Enantioselective Reductive Amination of $\alpha$ -Keto Acids to $\alpha$ -Amino Acids by a Pyridoxamine Cofactor in a Protein Cavity

Hao Kuang, Matthew L. Brown, Ronald R. Davies, Eva C. Young, and Mark D. Distefano\*

Contribution from the Department of Chemistry, University of Minnesota, Minneapolis, Minnesota 55455

Received December 21, 1995. Revised Manuscript Received August 9, 1996<sup>⊗</sup>

**Abstract:** Adipocyte lipid binding protein (ALBP) is a small 131 residue protein with a simple architecture that consists of two orthogonal planes of  $\beta$ -sheet secondary structure. This protein binds a variety of fatty acids in a large cavity formed between the two sheets such that the bound ligands are completely enclosed within the protein. In this paper, the synthesis of an ALBP conjugate (ALBP-PX) containing a pyridoxamine cofactor attached to a thiol within the protein interior is described. The conjugate was characterized by mass spectrometry, UV/vis spectroscopy, and gel filtration chromatography. ALBP-PX reductively aminates a number of alkyl, aryl, and side chain functionalized  $\alpha$ -keto acids to  $\alpha$ -amino acids with enantioselectivities as high as 94% *ee*.

## Introduction

Catalytic enantioselective reactions are of great importance in modern synthetic chemistry.<sup>1</sup> One strategy that can be used to design selective reaction catalysts is to incorporate nonspecific achiral catalytic molecules into chiral cavities. A number of cavities ranging from cyclodextrins to spherands have been exploited for this purpose.<sup>2</sup> Although successful in many cases, an important limitation of such systems is the difficulty involved in making incremental changes in the cavity size and shape. Small changes in cavity structure frequently involve major synthetic efforts. With the development of recombinant DNA technology and the concomitant capabilities it affords for protein manipulation, polypeptide based cavities offer tremendous potential. Several investigators have studied proteins derivitized with catalytic groups; however, most of the “semisynthetic enzymes” constructed to date have involved modifications on the surface or in clefts of the target proteins;<sup>3</sup> such systems do not allow the potential selectivity afforded by completely encapsulating the catalyst to be examined.

Adipocyte lipid binding protein (ALBP) is a small 131 residue protein with a simple architecture that consists of two orthogonal planes of  $\beta$ -sheet secondary structure.<sup>4</sup> A variety of fatty acids ranging from palmitate to arachidonate bind in a large (600 Å<sup>3</sup>) cavity formed between the two sheets.<sup>5</sup> An interesting feature of ALBP is that the bound ligands are completely enclosed within the protein; a space filling representation of the ALBP structure masks all atoms of the bound lipid.<sup>6</sup> Thus, ALBP possesses a true protein cavity and is a good system for evaluating the ability of protein cavities to affect the selectivity

of achiral catalysts; additionally, ALBP (and related proteins) has been the focus of numerous mutagenesis and protein folding studies which suggests that the protein cavity is amenable to modification.<sup>7</sup>

Pyridoxal and pyridoxamine are nonphosphorylated derivatives of cofactors that are involved in a number of important biological reactions including transaminations, racemizations, decarboxylations, and eliminations.<sup>8</sup> Since the reactions of these cofactors are well characterized and have been examined in a number of proteinaceous and non-proteinaceous systems,<sup>9,10</sup> we decided to study their reactivity and selectivity in the ALBP cavity. In this paper, the synthesis of an ALBP conjugate containing a pyridoxamine cofactor, attached to a thiol within the protein interior, and the reductive amination of seven  $\alpha$ -keto acids to amino acids by this construct are described. The study here focuses on enantioselectivity since the attainment of such selectivity remains one of the major challenges in modern synthetic chemistry.

## Results

**Design Considerations.** Our design for the desired ALBP conjugate originated with the observation that the thiol group from Cys<sub>117</sub> is located in the interior of the protein cavity; this unique cysteine residue has previously been modified with a variety of thiol-specific reagents.<sup>11</sup> These studies indicate that large, nonfatty acid molecules can be accommodated in the cavity

<sup>⊗</sup> Abstract published in *Advance ACS Abstracts*, October 1, 1996.

(1) Seebach, D. *Angew. Chem., Int. Ed. Engl.* **1990**, *29*, 1320.  
(2) (a) Dugas, H. *Bioorganic Chemistry*; Springer-Verlag New York, Inc.: New York, 1996. (b) Breslow, R. *Acc. Chem. Res.* **1995**, *28*, 146–153.  
(3) (a) Kaiser, E. T.; Lawrence, D. S. *Science* **1984**, *226*, 505–511. (b) Levine, H. L.; Nakagawa, Y.; Kaiser, E. T. *Biochem. Biophys. Res. Comm.* **1977**, *76*, 64–70. (c) Corey, D. R.; Schultz, P. G. *Science* **1987**, *238*, 1401–1403.  
(4) Xu, Z.; Bernlohr, D. A.; Banaszak, L. J. *Biochemistry* **1992**, *31*, 3484–3492.  
(5) LaLonde, J. M.; Bernlohr, D. A.; Banaszak, L. J. *Biochemistry* **1994**, *33*, 4885–4895.  
(6) Banaszak, L. J.; Winter, N.; Xu, Z.; Bernlohr, D. A.; Cowan, S.; Jones, T. A. *Adv. Protein Chem.* **1994**, *45*, 89–151.

(7) (a) Sha, R. S.; Xu, Z.; Banaszak, L. J.; Bernlohr, D. A. *J. Biol. Chem.* **1993**, *268*, 7885–7892. (b) Stump, D. G.; Lloyd, R. S.; Chytil, F. *J. Biol. Chem.* **1991**, *266*, 4622–4630. (c) Jiang, N.; Frieden, C. *Biochemistry* **1993**, *32*, 11015–11021. (d) Kim, K.; Cistola, D. P.; Frieden, C. *Biochemistry* **1996**, *35*, 7553–7558. (e) Cistola, D. P.; Kim, K.; Rogl, H.; Frieden, C. *Biochemistry* **1996**, *35*, 7559–7565.

(8) Martell, A. E. *Acc. Chem. Res.* **1989**, *22*, 115–124.

(9) (a) Breslow, R.; Hammond, M.; Lauer, M. *J. Am. Chem. Soc.* **1980**, *102*, 421–422. (b) Breslow, R.; Canary, J. W.; Varney, M.; Waddell, S. T.; Yang, D. *J. Am. Chem. Soc.* **1990**, *112*, 5121–5219. (c) Cochran, A. G.; Pham, T.; Sugasawara, R.; Schultz, P. G. *J. Am. Chem. Soc.* **1991**, *113*, 6672–6673. (d) Imperiali, B.; Roy, R. S. *J. Am. Chem. Soc.* **1994**, *116*, 12083–12084. (e) Kikuchi, J.-I.; Zhang, Z. Y.; Murakami, Y. *J. Am. Chem. Soc.* **1995**, *117*, 5383–5384.

(10) (a) Bruice, T. C.; Topping, R. M. *J. Am. Chem. Soc.* **1963**, *85*, 1480–1487. (b) Bruice, T. C.; Topping, R. M. *J. Am. Chem. Soc.* **1963**, *85*, 1488–1492. (c) Thanassi, J. W.; Butler, A. R.; Bruice, T. C. *Biochemistry* **1965**, *4*, 1463–1470.

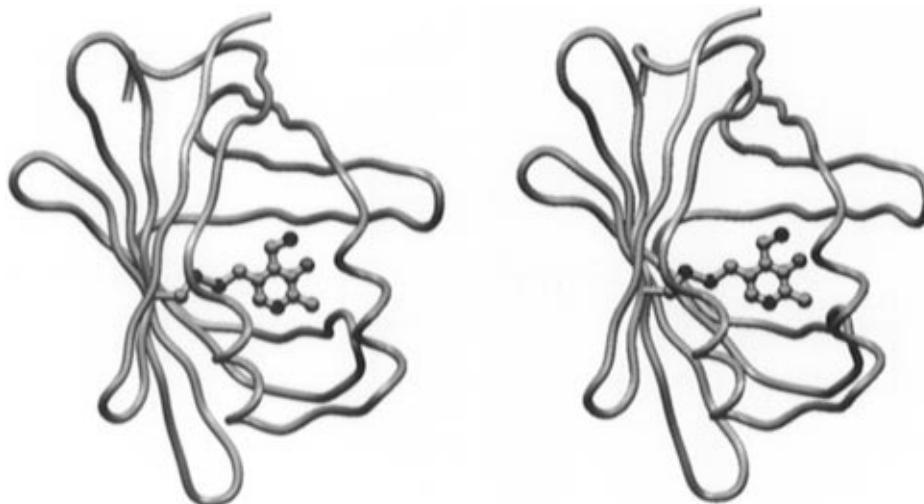


**Figure 1.** Stereoview of a model for the conjugate ALBP-PX showing pyridoxamine attached to a site in the protein interior. The overall fold of ALBP is shown in a ribbon representation with Cys<sub>117</sub> and the pyridoxamine shown in ball and stick format.

and that modification of Cys<sub>117</sub> does not result in large perturbations of the protein structure. Based on this knowledge, a model for an ALBP pyridoxamine conjugate (Figure 1) was constructed using the crystal structure of the ALBP/oleic acid complex.

**Preparation and Characterization of ALBP-PX.** To prepare the desired ALBP conjugate, **1** was first synthesized in five steps from pyridoxamine and purified by reversed-phase HPLC. ALBP was purified from an overproducing *E. coli* strain, JM105/pMON4 and was then reacted with compound **1** to generate the conjugate ALBP-PX (**2**). Thiol titration of the protein before and after reaction with **1** revealed the loss of 0.73 thiols per ALBP and indicated that the modification had occurred at Cys<sub>117</sub>. Analysis of ALBP-PX by electrospray mass spectrometry (Figure 2) indicated the presence of a new species

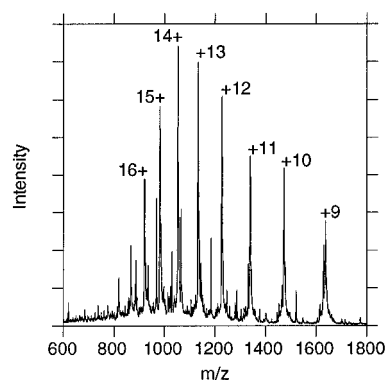
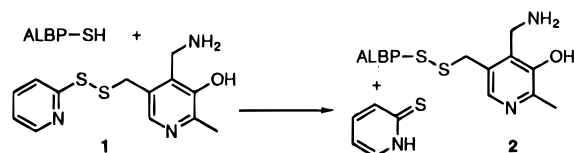


**Figure 2.** Electrospray mass spectrum of ALBP-PX. The charges of the peaks used to calculate the mass of ALBP-PX are noted on the plot.



with molecular mass 14 722.14 ( $\pm 2.94$ ) that compares well with the predicted value of 14 723.56 calculated for the conjugate. Spectrophotometric analysis of ALBP-PX after chromatography to remove unincorporated **1** revealed the presence of a new absorption band at 320 nm characteristic of pyridoxamine (spectrum A, Figure 3). While the extinction coefficient for this absorption band appeared low in the native conjugate, it increased significantly upon denaturation of ALBP-PX (spectrum B, Figure 3). Clearly, the microenvironment within the ALBP cavity perturbs the pyridoxamine chromophore and/or alters its protonation state. Comparison of the pyridoxamine concentration in ALBP-PX under denaturing conditions (calculated from a standard curve obtained for free pyridoxamine

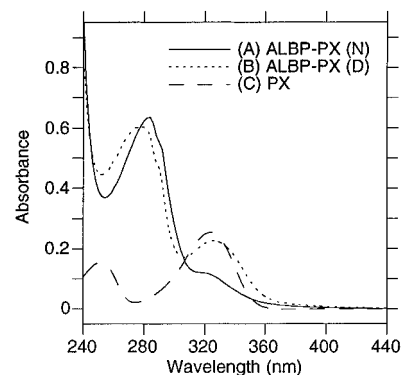


**Figure 3.** UV/vis spectra of ALBP-PX under native and denaturing conditions. (A) Spectrum of ALBP-PX (46  $\mu$ M) under native conditions. (B) Spectrum of ALBP-PX (46  $\mu$ M) under denaturing conditions. (C) Spectrum of 39  $\mu$ M pyridoxamine (85% of 46  $\mu$ M).

under the same conditions) with the total protein concentration in a sample of ALBP-PX (determined by protein assay) indicated that the modification reaction was 85% complete. This compared favorably with the thiol titration data described above and suggested that the desired conjugate had been prepared. Gel filtration chromatography (Figure 4) of ALBP and ALBP-PX under native conditions gave identical retention times suggesting that ALBP-PX maintains the folded structure present in the unmodified protein.

**Reactions Performed by ALBP-PX.** To examine the effect of the protein cavity on reaction selectivity, the reductive amination reactions shown below were studied. First, the initial

(11) Modification of this residue with bulky reagents blocks the binding of fatty acids: (a) Buelt, M. K.; Bernlohr, D. A. *Biochemistry* **1990**, *29*, 7408–7413. (b) Buelt, M. K.; Xu, Z.; Banaszak, L. J.; Bernlohr, D. A. *Biochemistry* **1992**, *31*, 3493–3499. Alkylation of thiols positioned in the cavity with fluorophores generates highly fluorescent derivatives: (c) Frieden, C.; Jiang, N.; Cistola, D. P. *Biochemistry* **1995**, *34*, 2724–2730. Both of these observations are consistent with modifications within the cavity.

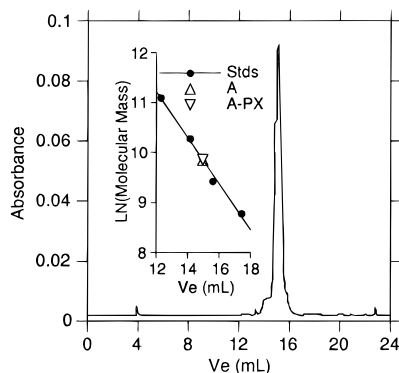


**Figure 4.** Gel filtration chromatography of ALBP-PX using a Superose 12 column. Inset: elution volume versus LN (molecular mass) of standard proteins used for the molecular mass determination of ALBP-PX. (I) Standards. ( $\Delta$ ) ALBP. ( $\nabla$ ) ALBP-PX.

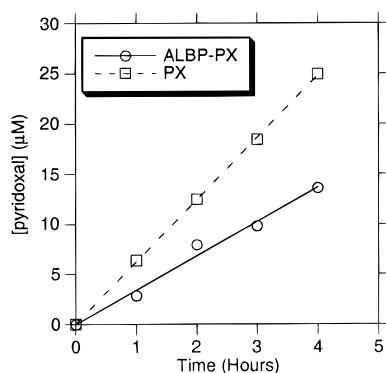
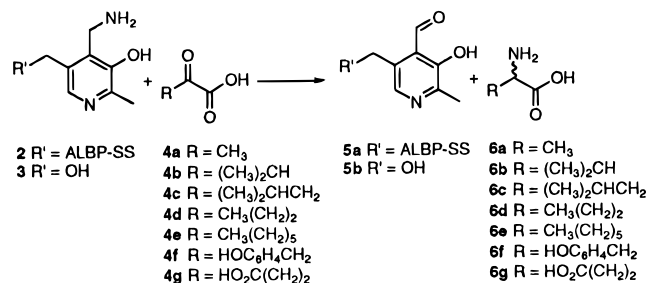


**Figure 5.** Initial rate data for the formation of pyridoxal from ALBP-PX or PX in the presence of pyruvate. (O) Rate data for the formation of pyridoxal from ALBP-PX. ( $\square$ ) Rate data for the formation of pyridoxal from pyridoxamine.

rates of reactions between pyruvate (**4a**) and PX (**3**) or ALBP-PX (**2**) were determined and are shown in Figure 5.<sup>12</sup> The rate of pyridoxal (**5b**) formation in the PX reaction was  $1.0 \times 10^{-7} \text{ M}\cdot\text{min}^{-1}$ , while the ALBP-PX reaction yielded the correspond-



ing aldehyde product (**5a**) at a rate of  $5.7 \times 10^{-8} \text{ M}\cdot\text{min}^{-1}$ . This 1.8-fold rate difference suggests that positioning the pyridoxamine catalyst in the ALBP cavity does not substantially affect the rate of the reaction.

The production of alanine (**6a**) in these two systems was examined next. The enantiomeric excess of amino acid products in the reactions was determined by forming diastereomeric fluorescent derivatives and separating and quantitating these derivatives by reversed-phase HPLC.<sup>13</sup> Reactions performed with PX produced no enantiomeric excess of D-alanine. In contrast, ALBP-PX produced a 42% *ee* of D-alanine after reacting for 24 h (18% conversion); a HPLC trace for this

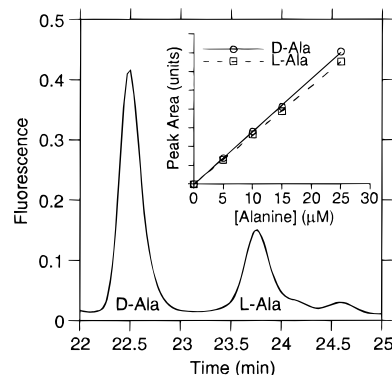


**Figure 6.** HPLC analysis of a reaction of ALBP-PX with pyruvate. Inset: calibration curve for the quantitation of D- and L-alanine showing that the fluorescence intensities for the two diastereomeric derivatives differ by 7.6%.

**Table 1.** Conversion and Enantioselectivities of ALBP-PX Reductive Amination Reactions

product	% conversion <sup>a</sup>	major enantiomer	% <i>ee</i>
alanine ( <b>6a</b> )	18 ± 3.6	D	42 ± 5.1
valine ( <b>6b</b> )	28 ± 1.9	L	94 ± 0.2
leucine ( <b>6c</b> )	39 ± 1.2	L	54 ± 0.8
norvaline ( <b>6d</b> )	21 ± 0.6	<sup>b</sup>	<sup>b</sup>
aminocaprylate ( <b>6e</b> )	13 ± 1.3	<sup>b</sup>	<sup>b</sup>
tyrosine ( <b>6f</b> )	42 ± 1.5	L	67 ± 7.3
glutamate ( <b>6g</b> )	46 ± 5.6	L	84 ± 2.2

<sup>a</sup> Conversion after 24 h. <sup>b</sup> No *ee* observed.

reaction is shown in Figure 6. Greater selectivity was obtained in reactions using a bulkier substrate,  $\alpha$ -keto isovalerate (**4b**), which produced valine (**6b**). In this case, a 77% *ee* for L-valine was obtained (24 h, 49% conversion). While performing the experiments with **4b** it was noticed that a small amount of precipitate had formed suggesting that ALBP-PX was aggregating or denaturing under the reaction conditions. To eliminate this problem, the ALBP-PX concentration was decreased from 156 to 50  $\mu\text{M}$ , and NaCl was added (20 mM, final concentration). Under these new conditions **6b** was produced from **4b** in 94% *ee* (24 h, 28% conversion). Keto acid **4c**, a  $\gamma$  branched substrate gave leucine (**6c**) in 54% *ee* (24 h, 39% conversion). Unbranched keto acid substrates **4d** (C<sub>5</sub>) and **4e** (C<sub>8</sub>) gave comparable levels of conversion to their respective amino acid products, **6d** and **6e**, but without any selectivity. A keto acid containing a phenolic side chain, **4f**, produced L-tyrosine (**6f**) in 67% *ee* (24 h, 42% conversion). A keto acid possessing a carboxylic acid side chain, **4g**, produced L-glutamate (**6g**) in 84% *ee* (24 h, 46% conversion). Conversions and selectivities for all the substrates studied are summarized in Table 1.

As a prelude to catalytic studies, the extent of product release in ALBP-PX mediated reactions was examined. Reactions between ALBP-PX and **4b** were performed, subjected to ultrafiltration, and analyzed by HPLC. The ultrafiltration step allowed the concentrations of free **6b** and **6b** bound to ALBP-PX to be determined. As summarized in Table 2, no significant amount of bound **6b** was observed.

## Discussion

The experiments described here suggest that the ALBP cavity can impart selectivity to reactions between pyridoxamine and a number of  $\alpha$ -keto acids with selectivities ranging from modest to excellent. The low *ee* observed with alanine is likely due to the small size of its side chain and its limited ability to serve as

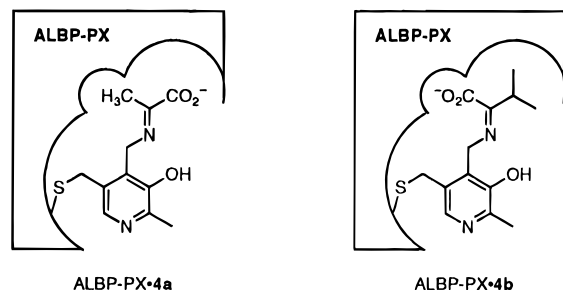
(12) Banks, B. E. C.; Diamantis, A. A.; Vernon, C. A. *J. Chem. Soc.* **1961**, 4135–4247.

(13) (a) Lindroth, P.; Mopper, K. *Anal. Chem.* **1979**, *51*, 1667–1674. (b) Nimura, N.; Kinoshita, T. *J. Chromatogr.* **1986**, *352*, 169–177. (c) Buck, R. H.; Krummen, K. *J. Chromatogr.* **1987**, *387*, 255–265.

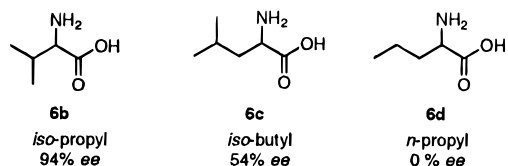
**Table 2.** Ultrafiltration Analysis of Valine Product from ALBP-PX Reactions

	reaction 1			reaction 2		
	[valine] ( $\mu$ M)	volume ( $\mu$ L)	ee (%)	[valine] ( $\mu$ M)	volume ( $\mu$ L)	ee (%)
before filtration	12.2		93.8	18.7		96.1
after filtration, top layer	14.0	20.1	94.5	16.9	17.6	96.2
after filtration, bottom layer	14.6	60.6	94.3	16.3	64.9	95.9

a directing group while the selectivity for the D enantiomer probably reflects a structural feature of the ketimine intermediate. If the largest substituent on the  $\alpha$  carbon controls the conformation about the imine linkage of the intermediate, then the stereochemical results obtained here (D for alanine, L for valine, leucine, tyrosine and glutamate) could result from preferential protonation from the same face in all cases; the results with alanine would simply reflect the unusual situation in which the amino acid side chain is smaller than the carboxyl group as shown below. The results observed with the alkyl



substituted  $\alpha$ -keto acids follow a trend where the selectivity is greatest when there is alkyl branching proximal to the developing chiral center. Valine (**6b**), with a  $\beta$ -methyl branch is produced in high *ee*, whereas leucine (**6c**) with its  $\gamma$ -methyl branch is generated in much lower *ee*; the nonbranched amino acids **6d** and **6e** are produced with no enantioselectivity. The ALBP-PX system appears to be quite general; a number of alkyl and aryl  $\alpha$ -keto acids as well as side chain functionalized  $\alpha$ -keto



acids are accepted. This is in contrast to results obtained with cyclodextrin based systems where only large substrates bind in the cavity.<sup>9a,b</sup> ALBP-PX does not accelerate the rate of amino acid production relative to free pyridoxamine in contrast to other cyclodextrin- and protein-based systems where 20–200-fold rate accelerations have been observed.<sup>9a,d</sup> This is probably due to both the lack of specific interactions between the substrate and conjugate, and the absence of rate-accelerating functional groups within the cavity. The low affinity exhibited by ALBP-PX for substrates appears to be mirrored in its product interactions. Ultrafiltration experiments indicate that amino acid products are predominantly free (unbound) and suggest that product release is not a problem in this system and that catalytic turnover should be possible. Additional experiments that examine the structural basis for the observed enantioselectivity via mutagenesis and crystallography and the ability to accomplish catalytic turnover are in progress. We conclude that protein cavities can be useful for the design of enantioselective catalysts and are using this approach for the design of other catalytic systems.<sup>14</sup>

(14) We have also prepared a conjugate of ALBP containing a Cu(II) phenanthroline moiety within the cavity. This protein catalyzes the enantioselective hydrolysis of amino acid esters.

## Experimental Section

**Purification of ALBP.** Large scale cultures of *E. coli* JM105/pMON4<sup>15</sup> were grown in LB Media to an O.D.<sub>600</sub> of 0.8 and induced with nalidixic acid. The cells were then grown for an additional 4 h, harvested by centrifugation, frozen in N<sub>2</sub> (l), and stored at –80 °C. For protein purification, 20 g of wet cell paste was resuspended in 50 mL of buffer A (25 mM imidazole-HCl, pH 7.0, 50 mM NaCl, 1 mM 2-mercaptoethanol, 5 mM EDTA, and 0.1 mM PMSF) and sonicated at 0 °C for 5 min. The resulting cell extract was then clarified by centrifugation, treated with 5 mL of 5% protamine sulfate in buffer A (w/v), and centrifuged to remove the precipitated nucleic acids. The supernatant was titrated to pH 5.0 with 2.0 M NaOAc, stirred overnight at 4 °C, centrifuged to remove precipitated proteins, and concentrated by ultrafiltration using a YM3 filter (Amicon). The solution of partially purified protein was then fractionated by chromatography on a Sephadex G-75 Superfine column (5 cm  $\times$  100 cm) equilibrated in buffer containing 12.5 mM HEPES, pH 7.5, and 0.25 M NaCl. The fractions were analyzed by SDS PAGE, and the pure fractions pooled and concentrated by ultrafiltration. Approximately 75 mg of pure protein was obtained. The purified protein was shown to be competent for high affinity fatty acid binding in titration experiments with fluorescent fatty acid analogs.<sup>7a</sup>

**Synthesis of 5-(2-Pyridyldithio)pyridoxamine (1).** Compound **1** was prepared by the reaction of 5-thiopyridoxamine dihydrobromide (synthesized in four steps from pyridoxamine dihydrochloride)<sup>16</sup> with 2,2'-dithiopyridine. A round bottom flask under a N<sub>2</sub> atmosphere was charged with 2,2'-dithiopyridine (661 mg, 3.0 mmol) dissolved in 15 mL of degassed MeOH. To this flask was added 5-thiopyridoxamine dihydrobromide (100 mg, 300  $\mu$ mol) dissolved in 5.7 mL of degassed MeOH, dropwise over 1 h. The solvent was removed *in vacuo*, and the yellow solid was washed three times with 10 mL of CHCl<sub>3</sub> and then dissolved in 2 mL of H<sub>2</sub>O/CH<sub>3</sub>CN (1/1, v/v) containing 0.2% TFA. The compound was purified by preparative reversed phase HPLC using a Rainin Dynamax Microsorb C<sub>18</sub> column (2.14  $\times$  25 cm with a 5 cm guard column). Chromatography was performed by injecting a 200  $\mu$ L sample and eluting with a flow rate of 10 mL/min and an elution profile consisting of isocratic elution with solvent A (H<sub>2</sub>O containing 5% CH<sub>3</sub>CN and 0.2% TFA) for 10 min followed by a 50 min linear gradient from 0% to 40% solvent B (CH<sub>3</sub>CN containing 0.2% TFA). Using this system, **1** eluted with a retention time of 32 min. Following chromatography, the fractions containing **1** were pooled and concentrated *in vacuo* to give 44 mg (48% yield) of a tan solid that darkened upon storage. Compound **1** stored at –20 °C is stable for several weeks but was found to be largely decomposed after 3 months. <sup>1</sup>H NMR (200 MHz, D<sub>2</sub>O)  $\delta$  8.25 (ddd, 1H, *J* = 5.4, 1.8, 0.8), 7.93 (s, 1H), 7.87 (ddd, 1H, *J* = 8.2, 7.6, 1.8), 7.61 (ddd, 1H, 8.2, 1.1, 1.1), 7.35 (ddd, 1H, *J* = 7.4, 5.5, 1.1), 4.26 (s, 2H), 4.14 (s, 2H), 2.35 (s, 3H); <sup>13</sup>C NMR (50.32 MHz, D<sub>2</sub>O)  $\delta$  157.4, 156.1, 146.6, 146.5, 144.7, 138.6, 136.6, 135.3, 127.4, 126.4, 38.3, 37.1, 17.2; HR-ESI MS calcd for C<sub>13</sub>H<sub>16</sub>N<sub>3</sub>OS<sub>2</sub> [M + H]<sup>+</sup>, 294.0734, found 294.0728.

**Synthesis of ALBP-PX.** ALBP (13 mg, 920 nmol) in 32 mL of 200 mM HEPES, pH 7.5, was mixed with **1** (2.7 mg, 9.2  $\mu$ mol) dissolved in H<sub>2</sub>O (65  $\mu$ L). The reaction was followed by monitoring the production of 2-thiopyridone spectrophotometrically at 342 nm and was complete after 30 min. It was then concentrated to 3 mL by ultrafiltration with a Centriprep 10 cartridge, applied to a BioGel P6-DG column (2.5  $\times$  16 cm), and eluted with 200 mM HEPES, pH 7.5, to remove unreacted **1** and 2-thiopyridone. The fractions containing ALBP-PX were then concentrated by ultrafiltration and the protein

(15) Xu, Z.; Buelt, M. K.; Banaszak, L. J.; Bernlohr, D. A. *J. Biol. Chem.* **1991**, *266*, 14367–14370.

(16) Breslow, R.; Czarnik, A. W.; Lauer, M.; Leppkes, R.; Winkler, J.; Zimmerman, S. *J. Am. Chem. Soc.* **1986**, *108*, 1969–1979.

concentration determined by the method of Bradford.<sup>17</sup> The final yield of the conjugate was 11 mg (84%). The extent of conjugation of ALBP by 1 was determined by thiol titration with 5,5'-dithiobis(2-nitrobenzoic acid) in 5.2 M guanidinium hydrochloride as described by Riddles et al.<sup>18</sup> and also by UV/vis spectrophotometry as described below.

**Electrospray Mass Spectrometry.** Samples for mass spectrometry were obtained by extensive dialysis of solutions of ALBP-PX in 200 mM HEPES (1 mL, 1.1 mg/mL) against H<sub>2</sub>O/MeOH/HOAc (89/10/1, v/v/v), (2 × 1 L). Spectra were obtained using a PE SCIEX API III MS/MS instrument, and the mass of ALBP-PX was determined by analysis of the intensity versus *m/z* data using HyperMass software.

**Gel Filtration Chromatography.** Gel filtration chromatography was performed using an FPLC system (Pharmacia) and a Superose 12 HR 30 column. Samples (100 μL) were eluted with 25 mM HEPES, pH 7.5, and 150 mM NaCl at a flow rate of 0.5 mL/min at 4 °C. The columns were calibrated using bovine lung aprotinin (6500 g/mol), horse heart cytochrome c (12 400 g/mol), bovine erythrocyte carbonic anhydrase (29 000 g/mol) and bovine serum albumin (66 000 g/mol).

**UV/vis Spectroscopy.** UV/vis spectra of ALBP-PX under native conditions were obtained using 46 μM ALBP-PX as determined by a Bradford protein assay in 200 mM HEPES, pH 7.5. Spectra of ALBP-PX under denaturing conditions contained 46 μM ALBP-PX, as determined above, and 4.8 M guanidinium hydrochloride in 200 mM HEPES, pH 7.5. Spectra of pyridoxamine were obtained at 39 μM (85% of 46 μM) in 200 mM HEPES, pH 7.5. The extinction coefficients ( $\epsilon_{322}$ ) for pyridoxamine in 200 mM HEPES, pH 7.5, and in the same buffer containing 4.8 M guanidinium hydrochloride were determined to be 7000 and 6100 M<sup>-1</sup> cm<sup>-1</sup>, respectively.

**Pyridoxal Formation Kinetics.** Reactions with the protein conjugate were performed using 157 μM ALBP-PX and 300 mM pyruvate in 200 mM HEPES, pH 7.5, in a final volume of 250 μL at 23 °C. At 1 h intervals, 45 μL samples were withdrawn from the reaction mixture and quenched with 45 μL of 50% aqueous ethanolamine (v/v) and 10 μL of 10% SDS (w/v). The amount of pyridoxal formed in the reaction was determined by spectrophotometric quantitation of its ethanolamine Schiff base adduct ( $\epsilon_{362} = 6740 \text{ M}^{-1} \text{ cm}^{-1}$ ) using a 100 μL ultramicrocuvette (Hellma) as described by Snell and Metzler.<sup>19</sup> The addition of SDS was used to denature the ALBP-PX and was necessary to obtain an accurate absorbance value for the Schiff base adduct. Under the conditions of the experiment, the SDS added altered the extinction coefficient for the Schiff base adduct by less than 5%. Reactions with pyridoxamine were performed using the concentrations described above in a 10 mL total volume. At 1 h intervals, 400 μL samples were withdrawn from the reaction mixture and quenched with 400 μL of 50% aqueous ethanolamine (v/v), and the pyridoxal product quantitated as described above.

**Reductive Amination Reactions.** All reactions were performed at 37 °C, terminated by flash freezing in N<sub>2</sub> (l), and stored at -80 °C prior to HPLC analysis. Reactions between pyruvate, **4a**, (0.3 M) and ALBP-PX (160 μM) or PX were performed in 200 mM HEPES, pH 7.5, in a total volume of 70 μL. Reactions between  $\alpha$ -keto isovalerate, **4b**, (0.3 M) and ALBP-PX (160 μM) were first performed in 200 mM HEPES, pH 7.5, in a total volume of 70 μL. After observing a precipitate in the reactions containing **4b**, the protein concentration was reduced to 50 μM and NaCl was added to a final concentration of 20 mM. The concentrations of the other components were as described above. Reactions between substrates **4c** through **4g** were performed with keto acid (50 mM) and ALBP-PX (50 μM) in 200 mM HEPES (pH 7.5) with 20 mM NaCl in a total volume of 100 μL.

**Derivatization.** Immediately before analysis, reaction samples were thawed and derivatized with 10 μL of a reagent consisting of *N*-acetyl-L-cysteine dissolved in "Incomplete *o*-Phthaldialdehyde Reagent Solution" (Sigma no. P7914) at a concentration of 5 mg/mL; these reagents convert enantiomeric amines into diastereomeric isoindoles. The derivatization reaction was allowed to proceed for 5 min at which time the sample was immediately analyzed by HPLC.

**HPLC Analysis.** All reaction mixtures were separated by reversed phase HPLC using a Rainin Microsorb-MV C<sub>18</sub> column (5 μm, 4.6 × 250 mm). Chromatography was performed by injecting a 10 μL sample

and eluting with a flow rate of 0.75 mL/min using a gradient of solvent A (80 mM sodium citrate and 20 mM sodium phosphate, pH 6.8) and solvent B (MeOH). Detection of the isoindole derivatives was achieved using a Beckman 6300A fluorescence detector (356 nm excitation filter and 450 nm emission filter) and integration was performed with a HP 3393A integrator or System Gold software. Response factors for the diastereomeric derivatives were obtained from calibration curves generated by derivatization and analysis of standard solutions of racemic amino acids. For alanine (**6a**), an elution profile consisting of isocratic elution with 80% solvent A for 5 min followed by a 10 min linear gradient from 20% to 40% solvent B and further elution with 60% solvent A was employed. Using this system, the retention times for the D- and L-alanine derivatives were 22.1 and 23.2 min, respectively. For valine (**6b**), an elution profile consisting of isocratic elution with 60% solvent A for 5 min followed by a 10 min linear gradient from 40% to 45% solvent B and further isocratic elution with 55% solvent A gave retention times for the L- and D-valine derivatives of 18.9 and 21.8 min, respectively. For tyrosine (**6f**), an elution profile consisting of isocratic elution with 70% solvent A for 5 min followed by a 5 min linear gradient from 30% to 35% solvent B and further isocratic elution with 65% solvent A giving retention times for the L- and D-tyrosine derivatives of 21.2 and 25.1 min, respectively. The amino acid derivatives discussed below were separated with a modified set of solvents consisting of solvent A (80 mM sodium citrate and 20 mM sodium phosphate, pH 6.8, containing MeOH, 10:1, v/v) and solvent B (MeOH). For leucine (**6c**), an elution profile consisting of isocratic elution with 60% solvent A for 5 min followed by a 5 min linear gradient from 40% to 50% solvent B and further isocratic elution with 50% solvent A gave retention times for the L- and D-leucine derivatives of 22.3 and 23.6 min, respectively. For norvaline (**6d**), an elution profile consisting of isocratic elution with 70% solvent A for 5 min followed by a 5 min linear gradient from 30% to 45% solvent B and further isocratic elution with 55% solvent A gave retention times for the norvaline derivatives of 25.2 and 26.1 min; respectively. For aminocaprylate (**6e**), an elution profile consisting of isocratic elution with 70% solvent A for 5 min followed by a 5 min linear gradient from 30% to 40% solvent B and further isocratic elution with 60% solvent A gave retention times for the aminocaprylate derivatives of 29.2 and 30.5 min, respectively. For glutamate (**6g**), the samples were eluted isocratically with 100% solvent A. Retention times for the L- and D-glutamate derivatives were 15.6 and 17.1 min, respectively.

**Ultrafiltration Experiments.** Two 100 μL solutions containing ALBP-PX (50 μM),  $\alpha$ -ketoisovaleric acid, **4b**, (0.3 M) and NaCl (20 mM) in HEPES (0.2 M, pH 7.5) were allowed to react for 24 h. Samples (10 μL) were withdrawn from each reaction and analyzed to determine the total valine concentration. The remaining sample from each reaction was then subjected to ultrafiltration with a Ultrafree-MC PLGC (Millipore) filter unit (10 000 nominal molecular mass limit for passage). The samples were centrifuged at 5000 × g for 10 min, and the volume of liquid in each layer was measured. Samples (10 μL) from the liquid above (top layer) and below (bottom layer) the filter along with the original 10 μL samples were then analyzed by HPLC (as described above) to determine the valine concentration. Similar experiments were performed with Ultrafree-MC PLCC (Millipore) and Centricon 3 (Amicon) filtration units that have 5000 and 3000 nominal molecular mass limits for passage, respectively.

**Acknowledgment.** The authors thank M. Silbergliitt for modeling ALBP-PX, L. Banaszak for providing the X-ray coordinates of ALBP, and D. Bernlohr for the plasmid pMON4. This work was supported by grants from the National Science Foundation (NSF-CHE-9506793) and the Petroleum Research Fund (PRF#28140-G4). M.L.B. was supported by the National Science Foundation REU program (NSF-CHE 9424203) and R.R.D. was supported by a National Institutes of Health Training Grant (NIH 2T32GM08347-06).

**Supporting Information Available:** <sup>1</sup>H NMR, <sup>13</sup>C NMR and HR-CIMS data for compound **1** (3 pages). See any current masthead page for ordering and Internet access instructions.

JA954271Z

(17) Bradford, M. M. *Anal. Biochem.* **1976**, *72*, 248–254.

(18) Riddles, P. W.; Blakeley, R. L.; Zerner, B. *Methods Enzymol.* **1983**, *91*, 49–59.

(19) Metzler, D. E.; Snell, E. E. *J. Am. Chem. Soc.* **1952**, *74*, 979–980.